ACS OMEGA

Article

Cite This: ACS Omega 2019, 4, 9964−9975

http://pubs.acs.org/journal/acsodf

Novel Inhibitory Function of the *Rhizomucor miehei* Lipase Propeptide and Three-Dimensional Structures of Its Complexes with the Enzyme

Olga V. Moroz,[†] Elena Blagova,[†] Verena Reiser,[‡] Rakhi Saikia,[§] Sohel Dalal,[§] Christian Isak Jørgensen,[‡] Vikram K. Bhatia,[‡,∥] Lone Baunsgaard,[‡] Birgitte Andersen,[‡] Allan Svendsen,[‡] and Keith S. Wilson*[,†]

[†]York Structural Biology Laboratory, Department of Chemistry, University of York, York YO10 5DD, U.K.

[‡]Novozymes A/S, Krogshøjvej 36, DK-2880 Bagsværd, Denmark

[§]Novozymes A/S, Plot No. 32, 47-50, Genisys Building, Whitefield, EPIP Zone, Brookefield, Bengaluru, Karnataka 560066, India

Supporting Information

ABSTRACT: Many proteins are synthesized as precursors, with propeptides playing a variety of roles such as assisting in folding or preventing them from being active within the cell. While the precise role of the propeptide in fungal lipases is not completely understood, it was previously reported that mutations in the propeptide region of the *Rhizomucor miehei* lipase have an influence on the activity of the mature enzyme, stressing the importance of the amino acid composition of this region. We here report two structures of this enzyme in complex with its propeptide, which suggests that the latter plays a role in the correct maturation of the enzyme. Most importantly, we demonstrate that the propeptide shows inhibition of lipase activity in standard lipase assays and propose that an important role of the propeptide is to ensure that the enzyme is not active during its expression pathway in the original host.

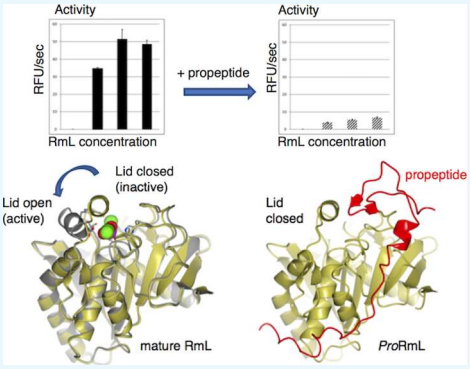

INTRODUCTION

The lipase from the fungus *Rhizomucor miehei* (henceforth, RmL refers to the mature enzyme, while *Pro*RmL refers to the proenzyme) belongs to the family of triglyceride lipases (EC 3.1.1.3) called class 3 lipases (PF01764 in Pfam, https://pfam.xfam.org),[1] which are members of the α/β hydrolase superfamily (53474 in SCOP, http://scop.mrc-lmb.cam.ac.uk/scop/)[2] that hydrolyze the ester linkages of triglycerides. Class 3 lipases are found in animals, plants, protists, and prokaryotes and are only distantly related to other lipase families. Their active sites were shown to contain a classical catalytic triad composed of Ser-His-Asp,[3] but in contrast to serine protease, the active sites are buried inside the structure. Subsequent structural studies revealed that there were two forms of RmL and related class 3 lipases: a closed inactive form that prevented access of the substrate to the active site and an open active form. The closed form is converted to the open conformation by the movement of a lid containing a short α-helix.[4]

Class 3 lipases, similar to a number of other proteins, contain an "additional" region during folding, which is subsequently cleaved either by autoprocessing, as is the case for several proteases, or by external proteases. These regions, termed propeptides, are often referred to as intramolecular chaperones (see ref 5 and references therein) and, as such, are required for proper folding and activity of the mature protein. Such an intramolecular chaperone was first described for subtilisin,[6] but they are found in various classes of prokaryotic and eukaryotic proteins, as reviewed in refs 7−9. X-ray structures have been determined for a number of propeptides containing proteins, particularly the proteases, as reviewed in ref 10.

The presence of a lipase propeptide was first reported for the enzyme from the fungus *R. miehei*,[11] where analysis of a complementary DNA library constructed in *Escherichia coli* revealed that the initial gene product is made up of domains corresponding to a 29-amino acid residue signal peptide, 65-residue N-terminal propeptide, and 269-residue mature enzyme (Figure 1).

While conventional prediction of the signal peptide length using the Signal 4.1 server (http://www.cbs.dtu.dk/services/SignalP/),[13] suggests cleavage occurs after residue 24; it appears that the final cleavage occurs after residue 29 in the pre-*Pro*RmL by a specific peptidase, KexB, which is an *Aspergillus oryzae* ortholog of *Saccharomyces cerevisiae* Kex2[14] that cleaves after KR (or RR) sequence motif during secretion in the Golgi.[15,16] Therefore, in our case, with the lipase being expressed in *A. oryzae*, as described below, the propeptide starts from residue 30.

Received: March 5, 2019
Accepted: May 13, 2019
Published: June 7, 2019

DOI: 10.1021/acsomega.9b00612
ACS Omega 2019, 4, 9964−9975

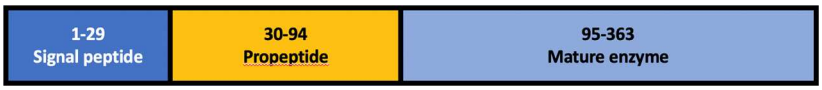

Figure 1. Components of pre-*Pro*RmL (UniProt P19515, PMID: 3419283) starting from residue 1 of the signal peptide. This residue numbering is used throughout the present communication; the original papers reporting the crystal structures of mature RmL[3,12] number this catalytic domain from 1 to 269, and thus, 94 needs to be added to those residue numbers when comparing them with those used here.

Early structural studies were undertaken on a *Rhizopus oryzae* (previously *Rhizopus delemar*) lipase with the aim of elucidating the propeptide function, but only the structure of the mature enzyme was reported[12] (PDB ID: 1TIC). Subsequently, there have been reports on the influence of mutations in the propeptide region on the enzyme activity of RmL[17,18] and on another class 3 lipase from *Thermomyces lanuginosus*, TLL;[19] however, there is no information available on the structure of the proenzyme or on the inhibitory effect of the propeptide. Bearing in mind the increasing body of evidence showing that mutations in the propeptide region can influence protein activity,[17,18] structural information on lipase propeptides is of interest for gaining a better understanding of the function of the class 3 lipases, will add to the growing body of propeptide information, and finally would be potentially applicable in improving the properties for industrially important processes.

The structure of mature RmL in the closed form was determined over 25 years ago.[3] Structures are now available for both the inactive, lid-closed and active, lid-open conformations[4] but were all restricted to the mature enzyme domain. We here report the first structures of RmL expressed in *Aspergillus* with its propeptide bound, derived from both a construct corresponding to the full-length proenzyme, that is residues 30−363 (the prolipase composed of the mature enzyme and propeptide domains), and a variant (henceforth, *Pro*RmL-del) of this proenzyme with two residues, 95 and 96, deleted. These structures suggest that one function of the propeptide is to bury the active site and binding area for the substrate before maturation. In addition, kinetics experiments are reported, which demonstrate the inhibitory effect of the propeptide when bound to the mature enzyme and allow us to propose a role for this inhibition in the natural host.

RESULTS AND DISCUSSION

Isolation of the Prolipase, Mature RmL, Propeptide, and Deletion Variant. Constructs were cloned and expressed as described in the Experimental Section. The identity of each of the samples was confirmed by mass spectrometry (Table 1).

Table 1. Only the Major Peak Is Shown[a]

sample	residue	theoretical MW	main measured MW
mature RmL	95−363	29,537.7	29,538.2
*Pro*RmL	30−363	36,228.0	N/A
cleaved propeptide	30−94	6708.3	6709.0
*Pro*RmL-del	30−361	36,027.7	36,028.4

[a]N/A, not available.

For the propeptide and *Pro*RmL-del, the measured values in the table have been corrected for the masses of expected posttranslational modifications.

1. *N*-acetylglucosamine at N-glycosylation site after *Endo*H deglycosylation (cleaved propeptide and *Pro*RmL-del).
2. Hexose at O-glycosylation site (cleaved propeptide and *Pro*RmL-del).
3. Pyroglutamic acid at N-terminal Gln(Q) (cleaved propeptide and *Pro*RmL-del).

Thus, purified samples were obtained for the following:

1. RmL, the mature wild-type enzyme without propeptide, residues 95−363.
2. *Pro*RmL, the wild-type prolipase, residues 30−363 (observed residues 95−363). This suggests that the propeptide has been cleaved from the mature enzyme and that this is a noncovalent complex of the propeptide bound to the mature enzyme.
3. Cleaved propeptide, separated from the mature enzyme, residues 30−94.
4. *Pro*RmL-del, the prolipase, residues 30−363 with residues 95−96 deleted.

Overall Fold. The structure of mature RmL was already known in its open and closed forms, and the closed form was used to solve crystal structures corresponding to the wild-type *Pro*RmL and the *Pro*RmL-del mutant samples by molecular replacement.

Wild-Type ProRmL Sample. The structure derived from the full-length wild-type *Pro*RmL sample was determined by molecular replacement using the closed form of the mature enzyme (PDB ID: 3TGL) as the search model. The final model is composed of residues 37−87 of the propeptide with a loop of residues 50−54 being disordered and with another missing region (88−97) with no electron density between the propeptide and the beginning of the mature enzyme. The density for the mature enzyme region starts at Gly98 and continues with no gaps until the C-terminal Thr363 (equivalent to residues 4−269 in the previously published mature RmL structures). The structure of the *Pro*RmL-del below had a smaller missing region, and hence, the discussion will focus on that structure. It is important to point out that the structure for the *Pro*RmL-del sample is very similar to that derived from the wild-type *Pro*RmL sample, indicating that the double mutation did not cause any significant changes to the overall fold.

The ProRmL-del Variant. The final model comprises residues 37−88 of the propeptide and 98−363 of the mature enzyme and is shown in Figure 2, superposed on the open and closed forms of the mature enzyme. It is immediately clear that the mature enzyme domain in the propeptide complex is in an essentially identical conformation to that in the closed form of the mature RmL (PDB ID: 3TGL), with an r.m.s. deviation over 264 equivalent Cα positions of 0.4 Å.

As expected, the novel feature in this structure is the presence of the propeptide, which wraps around the surface of the mature enzyme (Figure 2a,b). As stated above, the sequence in the previous PDB depositions was numbered from the first amino acid of the mature enzyme, while in the present structure, the numbering starts from the beginning of the signal peptide. This avoids negative residue numbers and means that

DOI: 10.1021/acsomega.9b00612
ACS Omega 2019, 4, 9964−9975

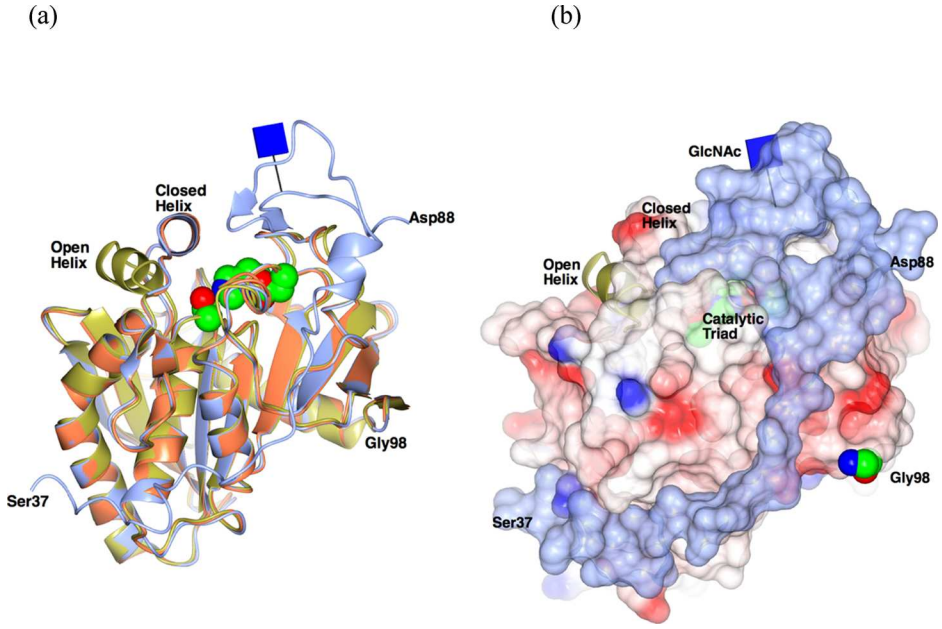

Figure 2. Overall structure of *Pro*RmL-del. (a) Superposition of the structure of *Pro*RmL-del (ice blue) on the mature RmL in its closed form (coral; PDB ID: 3TGL) and open form (gold; PDB ID: 4TGL). The single GlcNAc glycosylation site (Asn297) is shown in Glycoblock format.[20] The catalytic triad (Ser238, Asp297, and His351) is shown as spheres colored by the atom type. The distance between Asp88 and Gly98 is 24 Å. (b) Surface of *Pro*RmL-del, with the mature protein colored according to its electrostatic charge with transparency to reveal the buried catalytic triad (spheres), and the ordered propeptide Ser37-Asp88 in ice blue. The N-terminal residue of mature RmL, Gly98, is shown as spheres.

the residue numbers here correspond directly to the UniProt entry P19515.

There was well-defined electron density for the RmL propeptide residues 37−88 that revealed the structure of the propeptide for the first time, with no electron density for the first seven residues of the propeptide, which are assumed to be disordered. Residues 89−97 leading up to the first residue of the mature enzyme are also absent in the electron density map, implying that they are either cleaved despite all efforts to keep it intact or very flexible. It is not possible to state with confidence which of these two scenarios is true. Starting from Ser37, the propeptide wraps around the enzyme as an extended chain, leading up to a more compact segment making contacts with the lid of the mature enzyme (residues 178−186) through a number of interactions (Figure 2 and Table S1). The catalytic triad comprising the active site is seen to be buried below the compact domain of the propeptide (Figure 2). The propeptide packs against the α-helix which switches between open and closed conformations of the enzyme, maintaining the helix in the closed inactive position. The interactions of the propeptide with the lid will be discussed in more detail below.

The distance between the C-terminal ends of the ordered region of the propeptide, Asp88, and the first residue, Gly98, corresponding to the mature enzyme Gly4 is ∼24 Å. Before setting up the crystallization, the integrity of the *Pro*RmL-del sample was established from an SDS gel of the liquid in the drop containing crystals. Unfortunately, the crystals themselves have too small a volume to extract the protein and run the SDS gels or carry out mass spectrometric analysis. As stated above, it is therefore not clear whether residues 89−97 are disordered in the crystal or if this peptide has been cleaved during the crystal growth or, indeed, whether the cleaved protein has been selectively crystallized. It is also possible that a single cut has been made between residues 97 and 98 and that this has caused residues 89−97 to be disordered. The density around residues 88 and 97 is shown in Figure 3. A computer model of the full-length RmL propeptide was built using the X-ray structure of *Pro*RmL with the program Nest[21] from the Jackal 1.5 suite from Honig's group (Figure 3b) and clearly shows that the missing 10 residues can nicely span the gap between Asp88 and Gly98.

Binding of Propeptide to Mature RmL Leads to Inhibition of Activity. The RmL propeptide was separated from the *Pro*RmL sample. The isolated propeptide showed clear inhibition of activity in the GLAD lipase assay (an activity assay used for industrial applications that normally uses a high detergent level and hence required a high ratio of propeptide to mature RmL; public patent number: WO2016184944 (A1)) (Figure 4a). A propeptide fragment covering the lid-clip and hydrophobic anchor residues in the structure was found to interact quite strongly with the mature RmL in an aqueous binding assay. The independent measurement of the interaction between the propeptide and RmL gave an affinity (K_d) of 0.2 μM (Figure 4b). In the *Pro*RmL, the molar ratio is 1:1; thus, the measured low K_d of peptide binding bridges the inhibition study to the observations where neither *Pro*RmL nor *Pro*RmL-del shows a lipase activity in the zymogram area of the prominent bands representing the propeptide complex (see the Experimental Section, Figure 8).

We propose that the role of the propeptide is to ensure that there is no lipase activity during the expression pathway of the enzyme in the original host and that the enzyme only matures and becomes active late in the secretion pathway. Sequence alignment of a selected set of fungal lipases with similarity to RmL reveals a similarity in the propeptide region, indicating a general phenomenon of inhibition of unwanted activities during the expression of the lipase in the host cell. These results clearly demonstrate the inhibitory effect of the isolated propeptide and indicate the structural basis for the inhibition and lower binding to the purification material. (Covering of

DOI: 10.1021/acsomega.9b00612
ACS Omega 2019, 4, 9964−9975

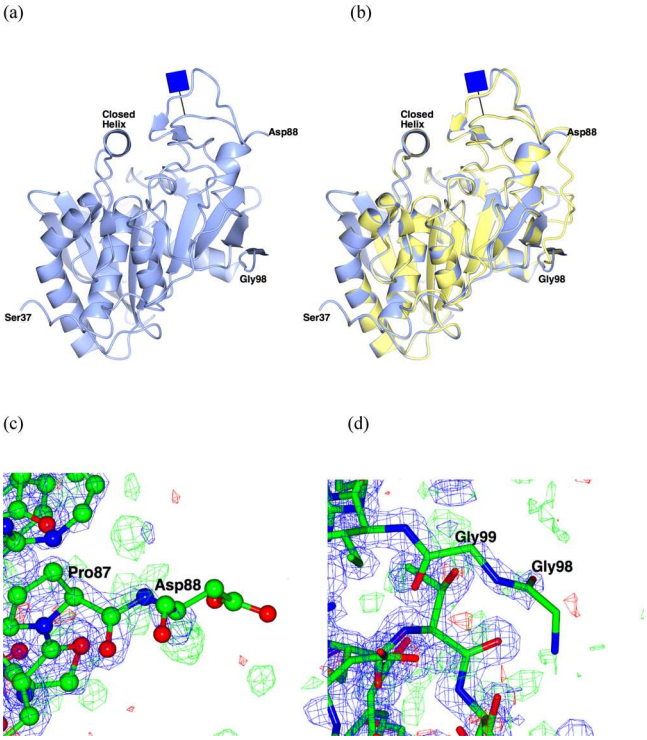

Figure 3. "Missing region", residues 88−97, in the *Pro*RmL-del structure. (a) Gap in the chain between Asp88 and Gly98: both residues point out into the disordered solvent. (b) Superposition of a computer model of the intact *Pro*RmL on the X-ray structure of the propeptide complex. The model was built starting from the X-ray structure of *Pro*RmL using the program Nest.[21] (c) Maximum likelihood density around Asp88 contoured at the 1.5σ level. (d) Same for Gly98. Indeed, the positions of part of Asp88 and Gly98 are only poorly defined with high *B* values.

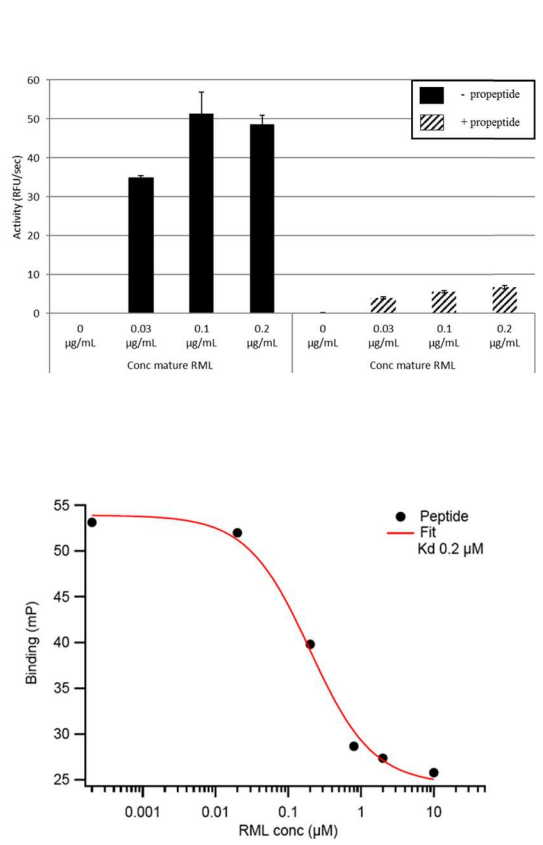

Figure 4. (a) Lipase activity assay after incubation of the mature RmL (left) without and (right) with addition of excess molar ratio of the purified propeptide. (b) Binding of the propeptide fragment to mature RmL, measured as a decrease in fluorescence polarization of the labeled peptide upon increasing concentration of RmL.

the hydrophobic anchor residue I250 and interaction with the lid in the closed form of the enzyme.)

Protein−Propeptide Interactions. The buried surface area between the propeptide and the mature enzyme is ~1771.2 Å^2 (analyzed using PISA,[23] corresponding to a strong protein−protein interaction).[24] The most significant interactions between the propeptide and mature enzyme from the PISA analysis are given in Table S1 (Supporting Information). In summary, there are 24 hydrogen bonds and five salt bridges, as well as hydrophobic interactions not given in Table S1. One of these interactions involves Leu81, which is one of the activity-related mutations identified in ref 17 and is a part of the hydrophobic cluster at the entrance to the active site, consisting of Ile183 from the lid and Val348. The mutation L81V leads to an increased activity, possibly because the contact between the mature enzyme and propeptide moiety is looser due to valine's smaller volume. (Several other activity-related substitutions reported by Wang and colleagues lie in the disordered regions with no visible electron density, so these cannot be interpreted structurally.[17,18]) The main chain oxygen of Leu81 forms a hydrogen bond to the main chain nitrogen of Val348, which further stabilizes the Leu-Val-Ile hydrophobic interaction holding the lid closed. Other direct interactions with the lid region include NZ of Lys76 to the main chain oxygens of Ala184 and Leu186 and OH of Tyr77 to the main chain nitrogen of Phe188 (Table S1 and Figure 7).

In addition to the lid interaction, the propeptide covers important hydrophobic regions of the mature lipase including surface-exposed I298, F345, and V348 while introducing a mostly hydrophilic surface. Residues forming hydrogen bonds inside and outside of the lid region are shown in Figure 5, which is a sequence alignment for several selected RmL-like lipases. There is only low sequence conservation for most of those, apparently because the majority of hydrogen bonds are from main chain atoms. However, Leu81 is conserved, with the corresponding residues being Leu in all but one of the sequences where it is Phe and is also hydrophobic. Another highly conserved proline-rich region is between residues 39 and 45 of *Pro*RmL, where the propeptide wraps around the mature domain.

In summary, the RmL propeptide is in contact with the lid and therefore reduces the contact for the lid to the lipid surface and, thus, its opening potential. This is supported by a structural similarity in the lid-covering region with another fungal lipase, RcL, as discussed below (Figure 7). The inhibition is probably dependent on two additional effects: (1) burying of one or more of the lipid-anchoring residues, that is, F345, V348, L349, and I298 (see Figure 6) and (2) adding a more hydrophilic surface on the rim of the lipase lid. Both potentially influence the penetration power of the lipase into the lipid surface and thus avoid the opening of the lid.

Thus, the *Pro*RmL structures show the propeptide covering a part of the area of the lipase that interacts with the lipid substrate surface (see Figure 6). A similar pattern is seen in the structure of a lipase with the same overall $\alpha\beta$-hydrolase fold, namely, that of the *Gibberella zeae* lipase (PDB ID: 3NGM)[25]

DOI: 10.1021/acsomega.9b00612
ACS Omega 2019, 4, 9964−9975

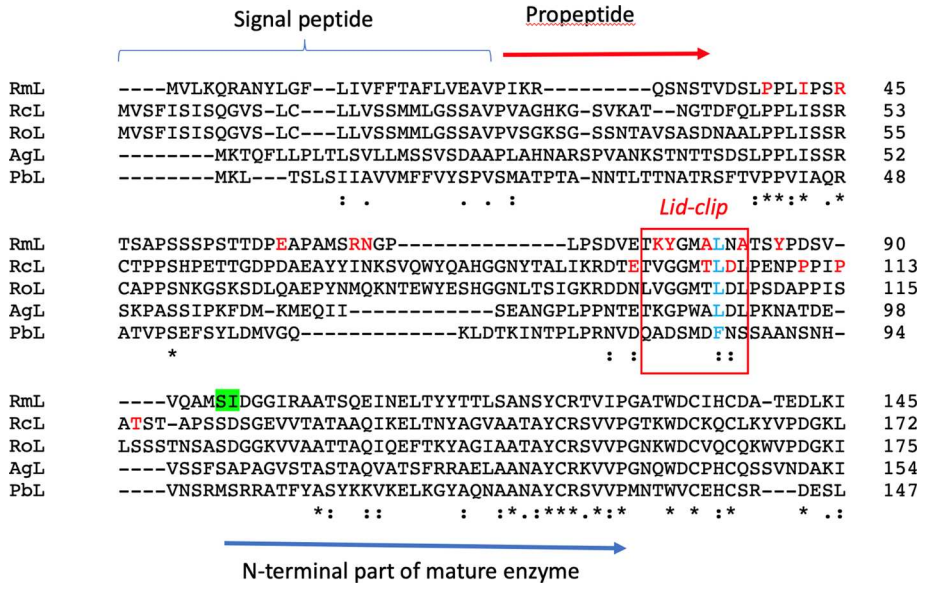

Figure 5. Alignment of several representative class 3 prolipase sequences for the propeptide regions and the beginning of the mature domain. The RmL-like sequences with a prepro sequence constitute lipases RmL (P19515; PDB IDs: 6QPP/6QPR; *R. miehei*), RcL (A3FM73; PDB ID: 4L3W; *Rhizopus chinensis*), P61872 (RoL, *R. oryzae*), AgL (A0A163J4P9, *Absidia glauca*), and PbL (A0A167LKQ2, *Phycomyces blakesleeanus*). The red box indicates the regions that are in contact with the lid of the mature enzyme domains (lid-clip) in the *Pro*RmL and *Pro*RcL X-ray structures. The residues of the propeptide that form hydrogen bonds or salt bridges with the mature domain are indicated in red. Leu81 in RmL (103 in RcL) that forms a hydrophobic interaction with Ile from the lid of the mature domain is shown in blue. The SI residues deleted in *Pro*RmL-del to prevent fast cleavage of the propeptide are outlined by the green box. The sequence alignment was done using ClustalOmega.[22]

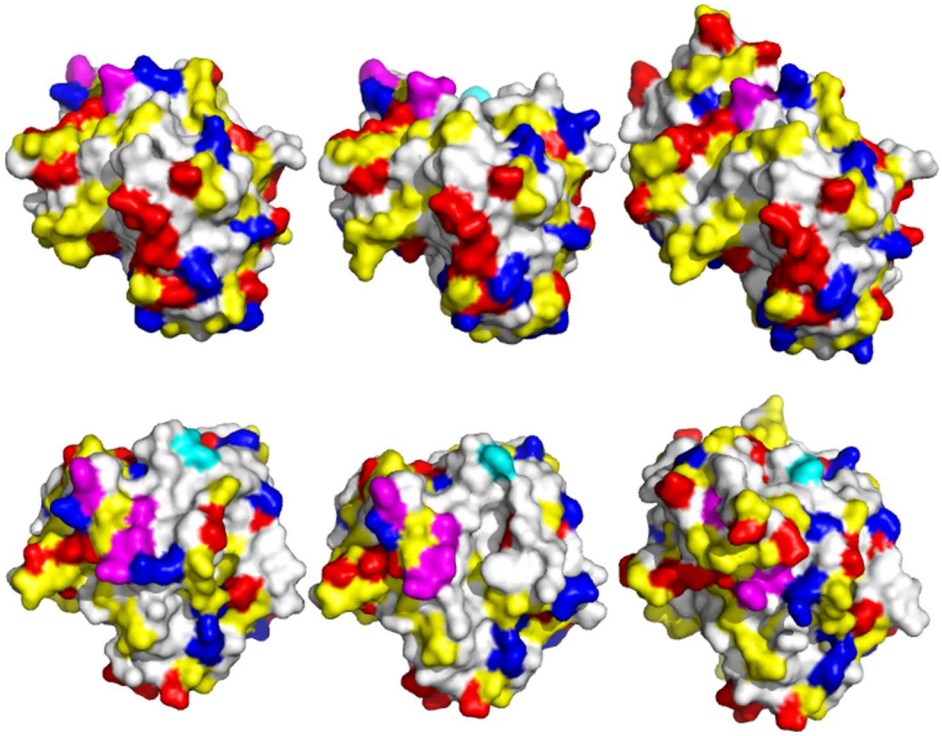

Figure 6. Surface representation of RmL and *Pro*RmL illustrating how the propeptide covers some of the hydrophobic residues in the lipid contact zone area of the closed RmL. From left to right, closed RmL, open RmL, and *Pro*RmL. Top row: View from the side with the lid on the top right. Bottom row: View into the lipid contact zone. Hydrophobic anchor-like residues in the surface exposed in the closed form are colored magenta (residue F345, V348, L349, and I298 in *Pro*RmL) or cyan. The only fully exposed F307 in *Pro*RmL (F213 in RmL) is colored cyan. All other hydrophobic residues are colored white, hydrophilic residues are yellow, positive residues are blue, and negative residues are red.

with a C-terminal extension covering a part of the same region as in *Pro*RmL just next to the lid of the two homologous lipases. The *G. zeae* enzyme belongs to the same sequence family as RmL but differs in having a C-terminal rather than an N-terminal propeptide attached. Interestingly, the location of the propeptide in two independent X-ray structures shows an interference of the two peptides in the same region of the functional part of the lipase. In sequences closely related to

DOI: 10.1021/acsomega.9b00612
ACS Omega 2019, 4, 9964−9975

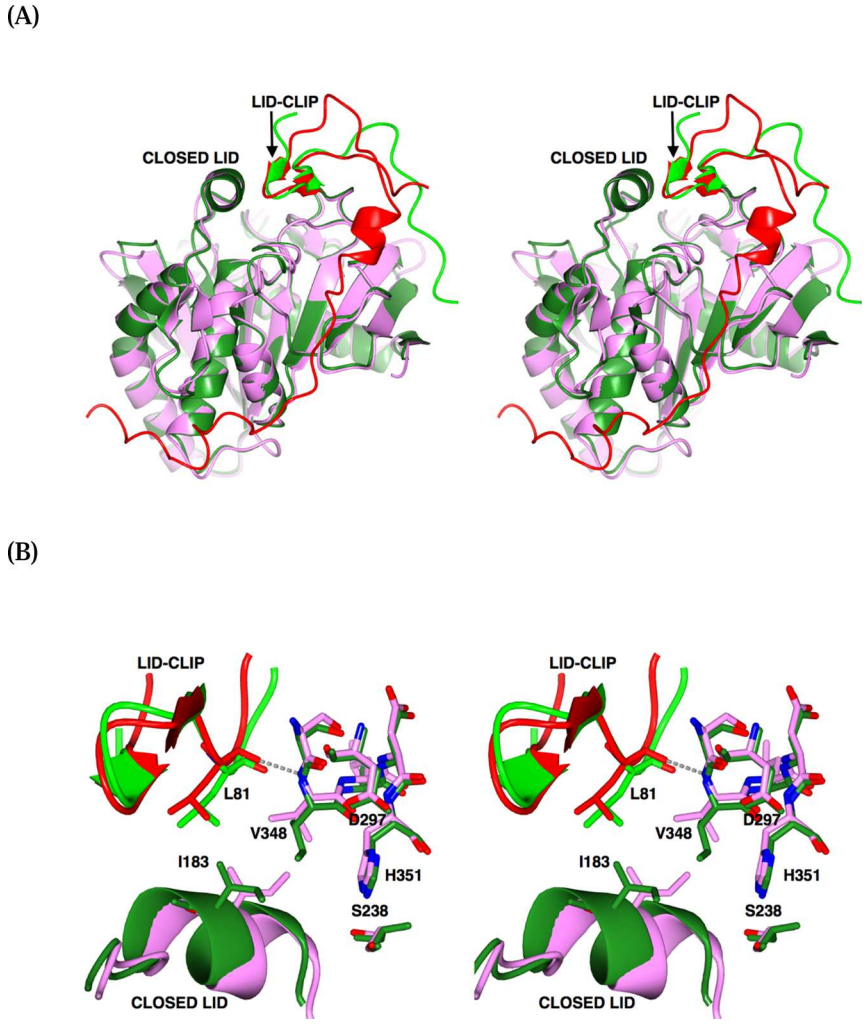

Figure 7. Stereo views of the superposition of *Pro*RmL-del and our re-refined model derived from 4L3W. (A) Overall superposition. The mature enzyme domains superimpose very well, and while propeptides (red for *Pro*RmL, green for 4L3W) have different conformations overall, the regions adjacent to the lid have a striking similarity. (B) Zoom-in on residues 73−83 (2−12 in 4L3W), showing details of the interactions preventing the lid from opening and thus protecting the binding site. Leu81 in *Pro*RmL-del (Leu103 in RcL) is involved in hydrophobic interactions with Ile183 (Ile210 in RcL) from the lid and is anchored to the main chain of the binding site by the hydrogen bond between its main chain O and N of Val348.

RmL, a certain promiscuity in activity can be seen, and for sequences closely related to *G. zeae*, many phospholipase-acting enzymes are seen.

Comparison to Lipase 4L3W: A Potential Propeptide in Another Lipase Structure. Analysis of the fungal lipase structures in the PDB led to an interesting and unexpected result. While, as discussed in the Introduction, no propeptide structure has been reported for fungal lipases to date, the structure of *Rhizopus microsporus* var. *chinensis* (RcL; PDB ID: 4L3W) contained an unusual chain of ethylene glycol molecules. Examination of the electron density maps from 4L3W in Coot revealed the presence of a probable polypeptide chain in the region modeled as ethylene glycols. We downloaded the coordinates, removed the chain of ethylene glycols, and re-refined the structure by adding the propeptide residues as described in the Experimental Section. This revealed a shorter visible propeptide than that from *Pro*RmL but with a very similar conformation to *Pro*RmL in the region 74−82 (96−104 in RcL) that covers the active site (Figure 7), with the sequence identity in this region being 50%. In particular, Leu81 (Leu103 in RcL) is conserved and forms a hydrophobic interaction with Ile183 (Ile210 in RcL), which belongs to the lid. Another hydrophobic residue in the vicinity of Leu81 (103) + Ile183 (210) is Val348 (Ile374 in RcL), which also has a hydrogen bond by the main chain nitrogen to the main chain oxygen of Leu81 (103) from the propeptide. This is a key interaction holding the lid in place and preventing its opening, and not surprisingly, Leu81 has been reported as one of the mutations influencing the protein activity.[17] The numbering for RcL is done in a way similar to what we use for RmL, that is, starting from the first residue of the signal peptide in the entry A3FM73.

CONCLUSIONS

Samples of mature *R. miehei* lipase, its prolipase form, *Pro*RmL, and cleaved propeptide were prepared. 3D structures from the *Pro*RmL samples for both the wild-type form and a variant with two residues deleted were determined using X-ray crystallography and revealed the structure of most of the propeptides with a small disordered region between the propeptide and mature enzyme domains. In the prolipase structure, the mature domain is in the closed inactive form, and this is stabilized by a

DOI: 10.1021/acsomega.9b00612
ACS Omega 2019, 4, 9964−9975

region of the propeptide that sits on top of the active site, preventing its opening. The remainder of the propeptide lies across the surface of the enzyme. The inhibition of the mature lipase by the propeptide when these two moieties are combined is demonstrated and confirmed the key inhibitory role of the propeptide in preventing the activation of the lipase during its expression. This is the first structure of a class 3 prolipase. In addition, we have reinterpreted the structure of a homologue from the PDB to suggest that it is also a prolipase with a similar mode of inhibition of its activity by the propeptide. We propose that the propeptide protects the cell in the course of its expression pathway to secure no lipase activity or, indeed, alternative activity such as phospholipase or glucolipid hydrolysis.

EXPERIMENTAL SECTION

Cloning, Expression, and Purification of Wild-Type *Pro*RmL. The gene for the wild-type *Pro*RmL was cloned and expressed in *A. oryzae*, as described previously.[11] The purification strategy was as follows. In the first step, the fermentation broth was applied to the hydrophobic interaction chromatography (HIC)/affinity column (decylamine that mimics a lipase substrate), and this procedure separated the active lipase (mature RmL without propeptide) from the inactive lipase (*Pro*RmL including the propeptide). After diafiltration, the inactive lipase was bound to an IEX column from which it was eluted and characterized to further purify and concentrate the sample. The active lipase was eluted from the HIC column and also characterized. A final purification was carried out for the stabilized *Pro*RmL, which was bound to a normal HIC column, since we knew that it would not bind to the HIC/affinity column. It was eluted and used for further experiments.

In more detail, the culture supernatant from the *A. oryzae* broth was first clarified by vacuum filtration using a combination of Seitz filter and Whatman glass filter GF/F grade in a Buchner funnel followed by sterile filtration using a Supor-200 0.2 μm filter on a vacuum filtration unit. The clarified culture supernatant was diluted 1:1 with 50 mM HEPES (pH 7) + 2 M NaCl. The decylamine column (15 × 200 mm; bed volume, 30 mL) was pre-equilibrated with wash buffer (50 mM HEPES (pH 7.0) + 1 M NaCl), and the sample was applied to the column at a linear flow rate of 8 mL/min. *Pro*RmL did not bind to the column and was collected from flow-through fractions, which were concentrated and then diafiltered against 50 mM HEPES (pH 7) buffer using a 10 kDa membrane in QuixStand TFF Unit. The final volume after diafiltration was 300 mL (conductivity, 5 mS/cm). This sample was directly loaded onto a UNO Q column (15 × 200 mm; bed volume, 21 mL) pre-equilibrated with 50 mM HEPES (pH 7.0) at a flow rate of 8 mL/min. Loosely bound impurities were removed by washing the column with 50 mM HEPES (pH 7.0) + 50 mM NaCl. The elution of *Pro*RmL was carried out using 50 mM HEPES (pH 7.0) and 1 M NaCl, and purified protein fractions were collected and pooled.

Isolation of Mature RmL. During the first step of the purification described above, after the flow-through containing *Pro*RmL was collected, the decylamine column was washed with 3 column volumes (CV) of buffer A (50 mM HEPES, (pH 7), 1 M NaCl), and the mature RmL without propeptide was then eluted in a step gradient of 3 CV 100% buffer B (Milli-Q water).

Native Gel and Parallel Zymogram on Purified RmL Samples. In addition to SDS PAGE, native PAGE followed by a zymogram was run to demonstrate the loss of activity in the propeptide-containing sample (Figure 8). The compositions

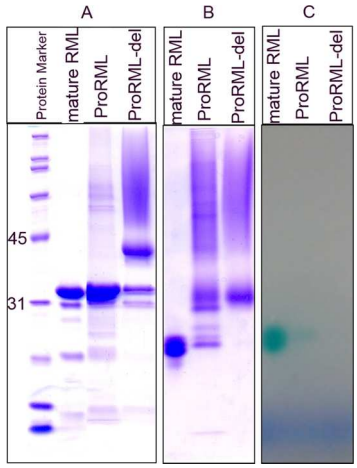

Figure 8. (A) 12% SDS PAGE, (B) native PAGE, and (C) zymogram of the native PAGE on purified mature RmL, purified wild-type *Pro*RmL, and purified *Pro*RmL-del. (A) SDS PAGE shows that mature RmL has a single strong band just above 31 kDa, and a prominent band with a similar size is observed in purified wild-type *Pro*RmL, whereas the prominent band in *Pro*RmL-del is just below the 45 kDa marker. In contrast, (B) native PAGE shows that wild-type *Pro*RmL has the most prominent band at a similar size as *Pro*RmL-del and a much weaker band at the size of mature RmL. (C) The zymogram based on the native PAGE only shows the lipase activity at the band corresponding to mature RmL, which is much stronger in mature RmL than in wild-type *Pro*RmL and absent in *Pro*RmL-del. Protein markers: 6.5, 14.4, 21.5, 31, 45, 66.2, 97.4, 116.25, and 200 MW.

for native PAGE were as follows. Resolving gel: 12% acrylamide-bis-acrylamide; 0.4 M Tris (pH 8.8), 0.1% APS, 0.04% TEMED. Stacking gel: 5.1% acrylamide-bis-acrylamide; 0.25 M Tris (pH 6.8), 0.1% APS, 0.1% TEMED. Loading dye: 0.06 M Tris (pH 6.8), 0.01% bromophenol blue, 10% glycerol. Running buffer: 3 g/L Tris base, 14.4 g/L glycine. Gel (B) is stained with brilliant blue. Zymogram: After electrophoresis, the native PAGE was placed on an agarose/brilliant blue plate (4% Litex HSB agarose protein grade, 50 mM HEPES (pH 7), 0.625% polyvinyl alcohol, 1.9% (v/v) olive oil, and 0.05% brilliant green (Sigma)).

Separation of *Pro*RmL from Mature RmL by Gel Filtration. Two hundred microliters of the mixture of *Pro*RmL and mature RmL was loaded on to a Superdex200 10/300 GL gel filtration column with a flow of 0.5 mL/min. The mobile phase was composed of 10 mM HEPES (pH 7) and 300 mM NaCl. The column was calibrated with an LMW gel filtration calibration kit (product code 28-4038-41, GE Healthcare Europe GmbH, Park Allé 295, 2605 Brondby, Denmark), and a linear relationship between the retention time and molecular weight was established according to the manual. The retention time of mature RmL is 16.9 min, which corresponds to a molecular weight of 27 kDa. The retention time of *Pro*RmL is 15.9 min, which corresponds to a molecular weight of 42 kDa. Thus *Pro*RmL is probably predominantly a cleaved propeptide−mature enzyme noncovalent complex (see SDS-PAGE (Figure 8) for the wild-type sample) but a covalent single

DOI: 10.1021/acsomega.9b00612
ACS Omega 2019, 4, 9964−9975

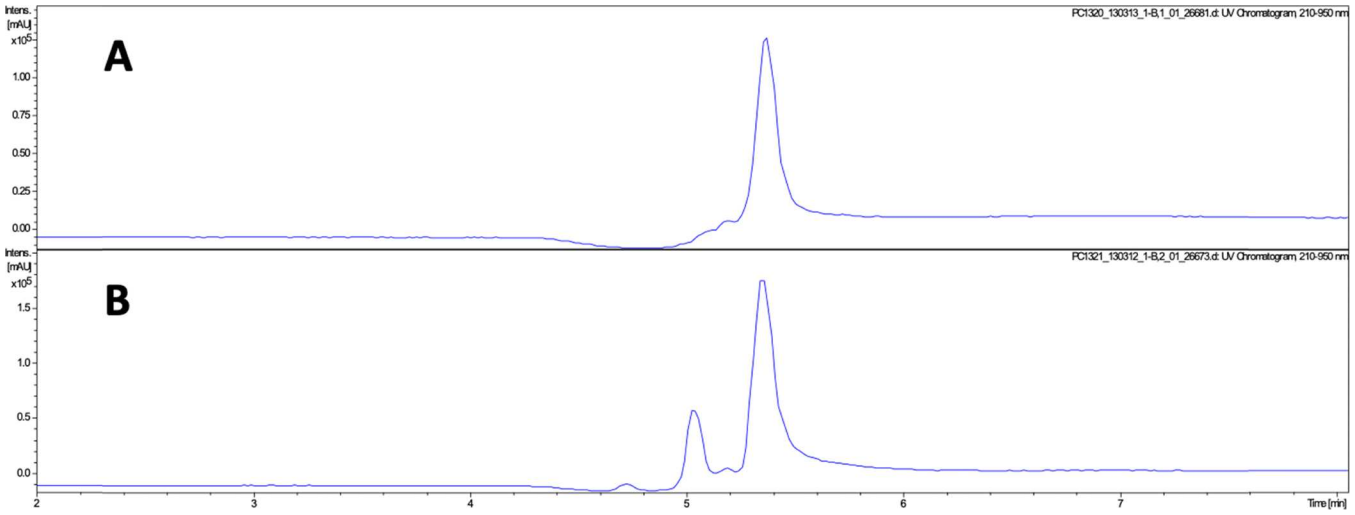

Figure 9. Chromatograms from the LC−MS experiment leading to the data in Table 1. Elution profiles of the two samples from the decylamine column during the HPLC C4 run in the LC−MS analysis. (A) Column binding fraction corresponding to mature RmL. (B) Nonbinding fraction that shows two peaks, the first being the cleaved propeptide and the second mature RmL. The association of the propeptide with the mature protein of the lipase appears to be noncovalent, indicating that wild-type *Pro*RmL is easily cleaved. Intact molecular weight analyses were performed using a MAXIS II electrospray mass spectrometer (Bruker Daltonik GmbH, Bremen, DE). The samples were first diluted to 0.1 mg/mL in MQ water. The diluted samples were applied to an AdvanceBio Desalting-RP column (Agilent Technologies) followed by washing and elution from the column running an acetonitrile linear gradient and introduced to the electrospray source with a flow of 400 mL/min by an Ultimate 3000 LC system (Dionex). Data analysis was performed with DataAnalysis version 4.3 (Bruker Daltonik GmbH, Bremen, DE).

moiety for *Pro*RmL-del. Samples from collected peaks from the gel filtration were subjected to mass spectrometry analysis (Figure 9).

Purification and Characterization of the RmL Propeptide. The RmL propeptide was separated from mature RmL in a two-step purification process at pH approximately 2.0−2.5. The starting material (unbound fraction from a hydrophobic interaction purification of the lipase) was diluted 20-fold in 10% (w/w) EtOH and 1% (w/w) formic acid and applied on a C8-silica resin (SP-200-15-C8-HP from Daiso Co., Ltd.). The column was washed with 10% (w/w) EtOH and 1% (w/w) formic acid, and the peptide was eluted as a very broad product peak with a linear gradient from 10% (w/w) EtOH and 1% (w/w) formic acid to 50% (w/w) EtOH and 1% (w/w) formic acid. RmL−propeptide-containing fractions as identified by peptide mapping by MS (next section) were combined and diluted 10-fold in dH_2O and applied on a C5-silica resin (C5 Jupiter 10 μm, 300 Å from Phenomenex). The column was washed with 10% (w/w) EtOH and 1% (w/w) formic acid, and the peptide was eluted as a broad product peak with a linear gradient from 10% (w/w) EtOH and 1% (w/w) formic acid to 50% (w/w) and 1% (w/w) formic acid. RmL−propeptide-containing fractions, as identified by peptide mapping by MS, were combined and dried in a centrifugal evaporator at room temperature. The dried material was dissolved in 50 mM Na-acetate (pH 4).

Protein identification was performed by tandem mass spectrometry (MS/MS) analysis of peptides released by protease digestion. Purified samples were first TCA-precipitated, and the protein pellet was then solubilized in a guanidine-HCL denaturation buffer heated with DTT for reduction of disulfide bonds, followed by alkylation with iodoacetamide. The samples were then washed and digested with a specific trypsin on a 10 kDa cutoff filter membrane. Following digestion, the resulting tryptic peptides were extracted and analyzed on an Orbitrap LTQ Velos Pro mass spectrometer (Thermo Scientific) where peptide masses and peptide fragment masses were measured.

The experimental masses were compared with the theoretical peptide values, and peptide fragment masses of proteins stored in databases using the mass search program Mascot (Matrix Science). In addition to the mature protein sequence, the data showed significant sequence coverage of the propeptide, residues −30−94.

Cloning, Expression, and Purification of the Deletion Variant: *Pro*RmL-del. With the aim of producing a more stable variant of *Pro*RmL, a construct, *Pro*RmL-del, was designed in which the first two residues, Ser95-Ile96, of the mature enzyme were deleted, as shown in the Results and Discussion section above. The specific cleavage was identified by MS analysis, and since no other significant cleavage sites were observed, it was assumed that cleavage is carried out by a specific endo-protease. Since the primary determinant for most endo-proteases is the P1 or P1′ position relative to the cleavage site, we aimed to remove the cleavage site by a double deletion of the P1 and P1′ amino acids. It was hoped that this variant would be resistant to automaturation and hence provide a stable form of the prolipase for structural and kinetics studies. PCR-based site-directed mutagenesis was used to generate variants with two overlapping primers, with the forward primer having the desired mutation in a single PCR reaction. The PCR product was treated with *Dpn*I restriction enzyme for 6 h at 37 °C, which digested the methylated or the parental template DNA, while the newly formed mutated DNA strands that were nonmethylated remained intact. The resulting PCR product was used to transform competent *E. coli* cells; the plasmid DNA was isolated (public patent number WO 2017/093318 PCT/EP2016/079277) from the single isolated transformants and sent for sequence analysis, which confirmed the presence of the desired mutation. The results confirmed that the plasmid DNA was transformed in *A. oryzae* ToC1512 by the protoplast mode. Transformants were screened for

DOI: 10.1021/acsomega.9b00612
ACS Omega 2019, 4, 9964−9975

protein expression on a small scale by inoculation of spores in 2 mL of expression media (M400) in 96-well culture plates and grown stationary for 4 days at 34 °C after which protein expression was analyzed on SDS-PAGE. The expressing colony was streaked on COVE-N-agar slants from which shake-flask fermentation was carried out in M400 media in 1 L of baffled shake flasks for 4 days at 34 °C and 180 rpm. Protein expression was analyzed by SDS-PAGE. Once the expression was confirmed, the fermentation broth was used for protein purification.

The culture supernatant from the *A. oryzae* broth was first clarified by vacuum filtration using a combination of Seitz filter and Whatman glass filter GF/F grade in a Buchner funnel, followed by sterile filtration using a Supor-200 0.2 μm filter on a vacuum filtration unit. Solid ammonium sulfate was added to the clarified broth to bring it to 1.5 M saturation, and the precipitates formed were removed by filtration. The sample was loaded on to a Butyl-Toyopearl column (15 × 200 mm; bed volume, 25 mL) pre-equilibrated with 25 mM HEPES (pH 7.0) + 1 M $(NH_4)_2SO_4$ at a flow rate of 5.5 mL/min. Unbound impurities were removed by washing with equilibration buffer.

Elution of *Pro*RmL-del including the propeptide (upper band on SDS-PAGE, Figure 2a) was carried out using 25 mM HEPES (pH 7) and 0.9 M $(NH_4)_2SO_4$. A second elution was performed using 0.8 M $(NH_4)_2SO_4$ and 0.2 M $(NH_4)_2SO_4$, which removed the majority of the impurities. Purified *Pro*RmL-del was subjected to Sephadex G-25 gel filtration column for desalting.

Inhibition of RmL by Its Propeptide. Inhibition of hydrolytic activity was determined by using the industrially relevant GLAD assay, measuring the release of 4-methyl-umbelliferone (4-MU) by purified mature RmL incubated with and without a propeptide (RmL−propeptide incubated at a molar ratio of 1:64) for 15 min in 0.2 M HEPES, 1 mM $CaCl_2$, and 10 ppm Triton X-100 (adjusted to pH 8.5). As a substrate, we used cellulose cotton linters, Avicel PH-101 (Sigma-Aldrich, 11365), uniformly coated with a 4.5:1 mixture of olive oil (Sigma-Aldrich, O-1514) and 4-methylumbelliferyl oleate (oleic acid 4-methylumbelliferyl ester (Sigma-Aldrich, 75164): 4 mg/mL in *n*-hexane (Sigma-Aldrich, 15671)). The coated cellulose fibers were suspended in 0.2 M HEPES, 3 mM $CaCl_2$, 0.5 mM $MgCl_2$, and 10 ppm Triton X-100 mixed with 3.3 g/L detergent solution using detergent model B (model B composition: 1% (w/w) NaOH, 7.2% (w/w) LAS, 3% (w/w) SLES, 5.5% (w/w) soy and coco fatty acids, 6.6% (w/w) AEO, 3.33% (w/w) triethanol amine, 2% (w/w) Na-citrate, 0.5% (w/w) DTMPA, 6% (w/w) MPG, 3% EtOH, 1.7% (w/w) glycerol, 1% (w/w) sodium formate, 0.1% (w/w) PCA; adjusted to pH 8.5) and RmL −/+ propeptide. The enzyme activity at room temperature was followed by measuring the fluorescence (kinetic mode) every 30 s at an excitation wavelength of 365 nm and emission wavelength of 445 nm from 1 to 6 min. The plate was only mixed by shaking for 5 s before the first measurement.

Propeptide Binding to Mature *R. miehei* Lipase. Binding was measured using fluorescence polarization (FP) and a Polarstar Omega instrument from BMG Labtech using a black 96-well plate (Nunc) and 100 μL assay volume. The peptide SDVETKYGMALNATSYC-A488 was synthesized by Schafer-N (Copenhagen, Denmark) at >95% purity, and purified mature RmL was used for measuring peptide binding. The fluorescent propeptide was diluted in HEPES buffer (50 mM HEPES (pH 7.5), 100 mM NaCl, 1 mM $CaCl_2$) to 0.9 μM and mixed with increasing concentrations of mature RmL (0.0002, 0.02, 0.2, 0.8, 2, and 10 μM) in duplicate. After incubating for 30 min at room temperature, the resulting steady-state equilibrium FP was detected in mP, and data were fitted to a Langmuir 1:1 model using Igor Pro (WaveMetrics).

Crystallization and Data Collection. *The Full-Length ProRmL Sample.* A cluster of plates was obtained in Hampton screen condition B3 (30% PEG8K, 0.1 M Na-cacodylate (pH 6.5), 0.2 M ammonium; Table 2). Data were collected at the Diamond Light Source, beamline I02, processed using MOSFLM[26] and scaled with Aimless.[27] The space group was *C*2, with cell dimensions a = 98.04 Å, b = 61.02 Å, c = 62.65 Å, and β = 111.97°. The data-processing statistics are given in Table 3.

Table 2. Crystallization

parameter	*Pro*RmL	*Pro*RmL-del
method	vapor diffusion, sitting drop	vapor diffusion, hanging drop
plate type	MRC two-well crystallization microplate, Swissci	Linbro 24-well
temperature (K)	293	
protein concentration	10 mg/mL	14 mg/mL
buffer composition of protein solution	10 mM HEPES, pH 7, 200 mM NaCl	25 mM HEPES, pH 7.0
composition of reservoir solution	30% PEG8K, 0.1 M Na-cacodylate, pH 6.5, 0.2 M ammonium sulfate	4 M Na formate
volume and ratio of drop	300 nL total, 1:1 ratio	1 μL total, 1:1 ratio
volume of reservoir	54 μL	1000 μL

The ProRmL-del Variant. Protease inhibitor cocktail (Pierce) was added straight after thawing the sample after transportation with the aim of preventing the cleavage of the propeptide. The protein was concentrated to 14 mg/mL in 25 mM HEPES (pH 7.0). Initial crystallization screening was carried out using sitting-drop vapor diffusion with drops set up using a Mosquito Crystal liquid-handling robot (TTP LabTech, U.K.), with 150 nL of protein solution and 150 nL of reservoir solution in 96-well format plates (MRC 2-well crystallization microplate, Swissci, Switzerland) equilibrated against 54 μL of reservoir solution. Experiments were carried out at room temperature with a number of commercial screens.

Initial crystals were obtained in Hampton condition C9 (4 M sodium formate) and were further optimized in a 24-well Linbro dish in hanging drop format. Final crystals were obtained in 4 M Na formate (the same reservoir content as the initial condition, but crystals were bigger and single after scale-up and addition of 0.1% β-octyl-glycoside to the protein) and were cryoprotected with 3.3 M Na malonate. The final crystallization drops were checked on an SDS gel to confirm that the intact propeptide was still present. Only the drop content could be checked; the crystals were too small to give an unambiguous result on a gel or by mass spectrometry. Final crystallization details are given in Table 2.

Data to 1.4 Å resolution were collected at the Diamond Light Source, beamline I04−1, processed using XDS[28] within the xia2 pipeline,[29] and scaled with Aimless.[27] The space group was *C*2, with cell dimensions a = 98.0 Å, b = 61.0 Å, c = 62.0 Å,

DOI: 10.1021/acsomega.9b00612
ACS Omega 2019, 4, 9964−9975

Table 3. Data Collection and Processing[a]

parameter	*Pro*RmL	*Pro*RmL-del
diffraction source	Diamond I02	Diamond I04-1
wavelength (Å)	0.98	0.92
temperature (K)	100	100
detector	Pilatus 6M-F	Pilatus 2M
crystal−detector distance (mm)	270	204.79
rotation range per image (°)	0.2	0.2
total rotation range (°)	220	220
exposure time per image (s)	0.2	0.2
space group	*C*2	*C*2
a, *b*, *c* (Å)	98.04, 61.02, 62.65	98.7, 61.4, 62.8
α, *β*, *γ* (°)	90, 111.97, 90	90, 111.85, 90
mosaicity (°)	0.29	0.23
resolution range (Å)	50.7−1.49 (1.53−1.49)	30.87−1.45 (1.47−1.45)
total no. of reflections	2,000,493 (1513)	207,794 (5543)
no. of unique reflections	55,513 (368)	58,551 (2028)
completeness (%)	99.2 (99.1)	95.0 (67.2)
redundancy	3.6 (3.6)	3.5 (2.7)
$CC_{(1/2)}$[b]	0.996 (0.893)	0.998 (0.797)
$\langle I/\sigma(I)\rangle$	9.8 (3.8)	13.8 (2.4)
R_{merge} (%)[c]	6.4 (27.0)	5.1 (40.8)
$R_{r.i.m.}$[d]	8.5 (36.4)	0.068 (0.559)
overall *B* factor from Wilson plot (Å^2)	14.1	8.6

[a]Values for the outer shell are given in parentheses. [b]$CC_{1/2}$ values for I_{mean} are calculated by splitting the data randomly in half. [c]R_{merge} is defined as $\Sigma|I - \langle I\rangle|/\Sigma I$, where I is the intensity of the reflection. [d]Redundancy-independent merging R factor $R_{r.i.m.}$ (Diederichs and Karplus, 1997).

Table 4. Structure Solution and Refinement[a]

parameter	WT *Pro*RmL	*Pro*RmL-del
resolution range (Å)	50.7−1.49 (1.53−1.49)	30.87−1.45 (1.47−1.45)
σ cutoff	3	2,
no. of reflections, working set	52,758	55606
no. of reflections, test set	2600	2797
final R_{cryst}	0.138	0.126
final R_{free}	0.178	0.165
Cruickshank DPI	0.0614	0.0561
no. of non-H atoms		
protein	2388	2461
sugar (NAG)	14	14
solute (EDO)	4	N/A
water	156	256
total	2562	2731
r.m.s. deviations		
bonds (Å)	0.017	0.017
angles (°)	1.869	1.985
average *B* factors (Å^2)	14.6	17.7
protein	13.9	16.7
sugar (NAG)	36.5	29.7
solute (EDO)	18.6	N/A
water	22.8	26.2
MolProbity score	0.81	1.08
Ramachandran plot		
most favored (%)	98.36	98.0
outliers (%)	0	0
PDB code	6QPP	6QPR

[a]Values for the outer shell are given in parentheses. N/A, not available.

and $\beta = 112°$. The data processing statistics are given in Table 3.

Structure Solution and Refinement. All computations were carried out using programs from the CCP4 suite,[30] unless otherwise stated.

The Wild-Type Full-Length ProRmL. The structure was solved using Molrep,[31] with the structure of mature RmL (3TGL) as a search model. The chain was traced with Buccaneer, and the model was refined with Refmac,[32] iterated with manual model correction using Coot.[33] The quality of the final model was validated using MolProbity[34] as part of the Phenix package.[35] The final refinement statistics are given in Table 4.

The ProRmL-del Variant. The structure was solved using Molrep,[31] with the structure of native full-length *Pro*RmL as a search model. Model building and refinement were carried out as described above for wild-type *Pro*RmL.

Analysis and Re-Refinement of *R. microsporus* var. *chinensis* Lipase. The coordinates and structure factors for *R. microsporus* var. *chinensis* lipase (PDB ID: 4L3W; henceforth, RcL) were downloaded from the PDB, together with the sequence from UniProt (entry A3FM73_RHICH). The structure contained the mature RcL and an extended feature modeled by the depositors as a set of ethylene glycol molecules. Inspection of the density suggested that the latter were in fact a region of the propeptide of RcL, and we edited the coordinates to remove ethylene glycols from the model. Residues from the propeptide were then built using Buccaneer, followed by refinement using Refmac and Coot. The modified structure is available in the Supporting Information.

Structure Comparisons. Structure comparisons were carried out using SSM,[36] as incorporated in CCP4mg.[37]

■ ASSOCIATED CONTENT

Supporting Information

The Supporting Information is available free of charge on the ACS Publications website at DOI: 10.1021/acsomega.9b00612.

Propeptide−mature protein interactions between individual residues, as output from PISA, and mass spectrometry analysis of the samples (PDF)

Coordinates of re-refined 4L3W in PDB format as a text file (PDB)

■ AUTHOR INFORMATION

Corresponding Author

*E-mail: keith.wilson@york.ac.uk. Tel.: +441904328262.

ORCID

Keith S. Wilson: 0000-0002-3581-2194

Present Address

[‖]Symphogen A/S, DK-2750 Ballerup, Denmark

DOI: 10.1021/acsomega.9b00612
ACS Omega 2019, 4, 9964−9975

Author Contributions

O.V.M. and E.B. carried out the crystal screening and structure analysis. O.V.M. co-wrote the paper. V.R. purified the *Pro*RmL and mature RmL and co-wrote the paper. R.S. and S.D. performed the experiments (variant generation, cloning, expression, purification) and co-wrote the article. C.I.J. planned and analyzed MS data and co-wrote the paper. V.K.B. performed the peptide binding experiment and co-wrote the paper. L.B. supervised the research at NZ; initiated, planned, and analyzed the in vitro lipase inhibition; and co-wrote the article. B.A. planned and analyzed the purification of the propeptide alone and co-wrote the paper. A.S. planned, designed, and supervised the NZ variant generation and co-wrote the article. K.S.W. supervised the structural biology and co-wrote the article.

Notes

The authors declare the following competing financial interest(s): Novozymes are a commercial enzyme supplier.

■ ACKNOWLEDGMENTS

The authors thank the Diamond Light Source for the access to beamlines I02 and I04-1 (proposals number mx-7864 and mx-9948) that contributed to the results presented here. The authors also thank Johan Turkenburg and Sam Hart for the assistance during data collection and Søren Hansen for assistance in assay development. All the Novozymes authors are employees of the company, and the York work is funded directly by Novozymes.

■ ABBREVIATIONS

RmL: mature *Rhizomucor miehei* lipase
KexB: specific peptidase from *Aspergillus oryzae*
TLL: *Thermomyces lanuginosus* lipase
*Pro*RmL: *Rhizomucor miehei* prolipase
*Pro*RmL-del: deletion mutant of *Rhizomucor miehei* prolipase
GlcNAc: *N*-acetyl-glucosamine
HEPES: 4-(2-hydroxyethyl)-1-piperazineethanesulfonic acid
SDS-PAGE: sodium dodecyl sulfate−polyacrylamide gel electrophoresis
MS: mass spectrometry

■ REFERENCES

(1) El-Gebali, S.; Mistry, J.; Bateman, A.; Eddy, S. R.; Luciani, A.; Potter, S. C.; Qureshi, M.; Richardson, L. J.; Salazar, G. A.; Smart, A.; Sonnhammer, E. L. L.; Hirsh, L.; Paladin, L.; Piovesan, D.; Tosatto, S. C. E.; Finn, R. D. The Pfam Protein Families Database in 2019. *Nucleic Acids Res.* **2019**, *47*, D427−D432.
(2) Andreeva, A.; Howorth, D.; Chandonia, J. M.; Brenner, S. E.; Hubbard, T. J.; Chothia, C.; Murzin, A. G. Data Growth and Its Impact on the Scop Database: New Developments. *Nucleic Acids Res.* **2008**, *36*, D419−25.
(3) Derewenda, Z. S.; Derewenda, U.; Dodson, G. G. The Crystal and Molecular Structure of the Rhizomucor Miehei Triacylglyceride Lipase at 1.9 a Resolution. *J. Mol. Biol.* **1992**, *227*, 818−39.
(4) Brzozowski, A. M.; Derewenda, U.; Derewenda, Z. S.; Dodson, G. G.; Lawson, D. M.; Turkenburg, J. P.; Bjorkling, F.; Huge-Jensen, B.; Patkar, S. A.; Thim, L. A Model for Interfacial Activation in Lipases from the Structure of a Fungal Lipase-Inhibitor Complex. *Nature* **1991**, *351*, 491−4.
(5) Chen, Y. J.; Inouye, M. The Intramolecular Chaperone-Mediated Protein Folding. *Curr. Opin. Struct. Biol.* **2008**, *18*, 765−70.
(6) Ikemura, H.; Takagi, H.; Inouye, M. Requirement of Pro-Sequence for the Production of Active Subtilisin E in Escherichia Coli. *J. Biol. Chem.* **1987**, *262*, 7859−64.
(7) Eder, J.; Fersht, A. R. Pro-Sequence-Assisted Protein Folding. *Mol. Microbiol.* **1995**, *16*, 609−14.
(8) Shinde, U.; Inouye, M. Intramolecular Chaperones: Polypeptide Extensions That Modulate Protein Folding. *Semin. Cell Dev. Biol.* **2000**, *11*, 35−44.
(9) Baker, D.; Shiau, A. K.; Agard, D. A. The Role of Pro Regions in Protein Folding. *Curr. Opin. Cell Biol.* **1993**, *5*, 966−70.
(10) Demidyuk, I. V.; Shubin, A. V.; Gasanov, E. V.; Kostrov, S. V. Propeptides as Modulators of Functional Activity of Proteases. *Biomol. Concepts* **2010**, *1*, 305−22.
(11) Boel, E.; Huge-Jensen, B.; Christensen, M.; Thim, L.; Fiil, N. P. Rhizomucor Miehei Triglyceride Lipase Is Synthesized as a Precursor. *Lipids* **1988**, *23*, 701−6.
(12) Derewenda, U.; Swenson, L.; Wei, Y.; Green, R.; Kobos, P. M.; Joerger, R.; Haas, M. J.; Derewenda, Z. S. Conformational Lability of Lipases Observed in the Absence of an Oil-Water Interface: Crystallographic Studies of Enzymes from the Fungi Humicola Lanuginosa and Rhizopus Delemar. *J. Lipid Res.* **1994**, *35*, 524−34.
(13) Nielsen, H. Predicting Secretory Proteins with Signalp. *Methods Mol. Biol.* **2017**, *1611*, 59−73.
(14) Mizutani, O.; Nojima, A.; Yamamoto, M.; Furukawa, K.; Fujioka, T.; Yamagata, Y.; Abe, K.; Nakajima, T. Disordered Cell Integrity Signaling Caused by Disruption of the Kexb Gene in Aspergillus Oryzae. *Eukaryotic Cell* **2004**, *3*, 1036−48.
(15) Fuller, R. S.; Brake, A.; Thorner, J. Yeast Prohormone Processing Enzyme (Kex2 Gene Product) Is a Ca2+−Dependent Serine Protease. *Proc. Natl. Acad. Sci. U. S. A.* **1989**, *86*, 1434−8.
(16) Redding, K.; Holcomb, C.; Fuller, R. S. Immunolocalization of Kex2 Protease Identifies a Putative Late Golgi Compartment in the Yeast Saccharomyces Cerevisiae. *J. Cell Biol.* **1991**, *113*, 527−38.
(17) Wang, J.; Wang, D.; Wang, B.; Mei, Z. H.; Liu, J.; Yu, H. W. Enhanced Activity of Rhizomucor Miehei Lipase by Directed Evolution with Simultaneous Evolution of the Propeptide. *Appl. Microbiol. Biotechnol.* **2012**, *96*, 443−450.
(18) Wang, Z.; Lv, P.; Luo, W.; Yuan, Z.; He, D. Expression in Pichia Pastoris and Characterization of Rhizomucor Miehei Lipases Containing a New Propeptide Region. *J. Gen. Appl. Microbiol.* **2016**, *62*, 25−30.
(19) Cai, H.; Zhao, M.; Li, Y.; Mao, J.; Cai, C.; Feng, F. Pentapeptide Prosequence Enhances Expression and Structure Folding of Recombinant Thermomyces Lanuginosus Lipase in Pichia Pastoris. *Protein Pept. Lett.* **2017**, *24*, 676−681.
(20) McNicholas, S.; Agirre, J. Glycoblocks: A Schematic Three-Dimensional Representation for Glycans and Their Interactions. *Acta Crystallogr., Sect. D: Struct. Biol.* **2017**, *73*, 187−194.
(21) Petrey, D.; Xiang, Z.; Tang, C. L.; Xie, L.; Gimpelev, M.; Mitros, T.; Soto, C. S.; Goldsmith-Fischman, S.; Kernytsky, A.; Schlessinger, A.; Koh, I. Y.; Alexov, E.; Honig, B. Using Multiple Structure Alignments, Fast Model Building, and Energetic Analysis in Fold Recognition and Homology Modeling. *Proteins: Struct., Funct., Bioinf.* **2003**, *53*, 430−5.
(22) Sievers, F.; Wilm, A.; Dineen, D.; Gibson, T. J.; Karplus, K.; Li, W.; Lopez, R.; McWilliam, H.; Remmert, M.; Söding, J.; Thompson, J. D.; Higgins, D. G. Fast, Scalable Generation of High-Quality Protein Multiple Sequence Alignments Using Clustal Omega. *Mol. Syst. Biol.* **2011**, *7*, 539.
(23) Krissinel, E. Stock-Based Detection of Protein Oligomeric States in Jspisa. *Nucleic Acids Res.* **2015**, *43*, W314−9.
(24) Janin, J.; Bahadur, R. P.; Chakrabarti, P. Protein-Protein Interaction and Quaternary Structure. *Q. Rev. Biophys.* **2008**, *41*, 133−80.
(25) Lou, Z.; Li, M.; Sun, Y.; Liu, Y.; Liu, Z.; Wu, W.; Rao, Z. Crystal Structure of a Secreted Lipase from Gibberella Zeae Reveals a Novel "Double-Lock" Mechanism. *Protein Cell* **2010**, *1*, 760−70.
(26) Leslie, A. G. The Integration of Macromolecular Diffraction Data. *Acta Crystallogr., Sect. D: Biol. Crystallogr.* **2006**, *62*, 48−57.

DOI: 10.1021/acsomega.9b00612
ACS Omega 2019, 4, 9964−9975

(27) Evans, P. R.; Murshudov, G. N. How Good Are My Data and What Is the Resolution? *Acta Crystallogr., Sect. D: Biol. Crystallogr.* **2013**, *69*, 1204−14.
(28) Kabsch, W. Xds. *Acta Crystallogr., Sect. D: Biol. Crystallogr.* **2010**, *66*, 125−32.
(29) Winter, G.; Lobley, C. M. C.; Prince, S. M. Decision Making in Xia2. *Acta Crystallogr. D* **2013**, *69*, 1260−1273.
(30) Winn, M. D.; Ballard, C. C.; Cowtan, K. D.; Dodson, E. J.; Emsley, P.; Evans, P. R.; Keegan, R. M.; Krissinel, E. B.; Leslie, A. G. W.; McCoy, A.; McNicholas, S. J.; Murshudov, G. N.; Pannu, N. S.; Potterton, E. A.; Powell, H. R.; Read, R. J.; Vagin, A.; Wilson, K. S. Overview of the Ccp4 Suite and Current Developments. *Acta Crystallogr. D* **2011**, *67*, 235−242.
(31) Vagin, A.; Teplyakov, A. Molecular Replacement with-MOLREP. *Acta Crystallogr. D* **2010**, *66*, 22−25.
(32) Murshudov, G. N.; Skubak, P.; Lebedev, A. A.; Pannu, N. S.; Steiner, R. A.; Nicholls, R. A.; Winn, M. D.; Long, F.; Vagin, A. A. Refmac5 for the Refinement of Macromolecular Crystal Structures. *Acta Crystallogr., Sect. D: Biol. Crystallogr.* **2011**, *67*, 355−367.
(33) Emsley, P.; Lohkamp, B.; Scott, W. G.; Cowtan, K. Features and Development of Coot. *Acta Crystallogr., Sect. D: Biol. Crystallogr.* **2010**, *66*, 486−501.
(34) Chen, V. B.; Arendall, W. B., 3rd; Headd, J. J.; Keedy, D. A.; Immormino, R. M.; Kapral, G. J.; Murray, L. W.; Richardson, J. S.; Richardson, D. C. Molprobity: All-Atom Structure Validation for Macromolecular Crystallography. *Acta Crystallogr., Sect. D: Biol. Crystallogr.* **2010**, *66*, 12−21.
(35) Adams, P. D.; Afonine, P. V.; Bunkoczi, G.; Chen, V. B.; Echols, N.; Headd, J. J.; Hung, L. W.; Jain, S.; Kapral, G. J.; Grosse Kunstleve, R. W.; McCoy, A. J.; Moriarty, N. W.; Oeffner, R. D.; Read, R. J.; Richardson, D. C.; Richardson, J. S.; Terwilliger, T. C.; Zwart, P. H. The Phenix Software for Automated Determination of Macromolecular Structures. *Methods* **2011**, *55*, 94−106.
(36) Krissinel, E.; Henrick, K. Secondary-Structure Matching (Ssm), a New Tool for Fast Protein Structure Alignment in Three Dimensions. *Acta Crystallogr., Sect. D: Biol. Crystallogr.* **2004**, *60*, 2256−68.
(37) McNicholas, S.; Potterton, E.; Wilson, K. S.; Noble, M. E. M. Presenting Your Structures: The Ccp4mg Molecular-Graphics Software. *Acta Crystallogr., Sect. D: Biol. Crystallogr.* **2011**, *67*, 386−94.

DOI: 10.1021/acsomega.9b00612
ACS Omega 2019, 4, 9964−9975